A THEORETICAL AND EXPERIMENTAL STUDY

OF THE ROLL CASTING PROCESS

R. J. O'MALLEY AND M. E. KARABIN

ALUMINUM COMPANY OF AMERICA
ALCOA LABORATORIES
ALCOA CENTER, PA 15069

Abstract

A mathematical model of the roll casting process has been developed which predicts macro-variables, such as roll separating force, roll torque, and strip exit speed for a range of roll speeds. Continuum variables, such as interface pressure, interface shear stress, freeze-front shape, and internal temperature distribution are also predicted.

The model consists of two independent segments: solidification and rolling. The solidification model is two-dimensional (thickness and rolling direction) and is capable of handling alloy solidification. The solidification model is employed until solidification through the thickness is complete, then the rolling solution is activated.

The rolling model is a one-dimensional (rolling direction) mechanical solution based on the von Karman approach, coupled with a two-dimensional thermal solution. The flow stress is expressed as a function of the average through-thickness temperature of the strip.

Experiments were performed using a laboratory roll caster to test and refine the model. Experimental strip exit temperatures were used as input to the model. Experimental and predicted roll torque and strip exit speed were forced into agreement at a single reference roll speed to obtain values for the coefficient of friction and the interfacial heat transfer coefficient. Using these values, good agreement was obtained between predicted and experimental torque and strip exit speed over the entire range of roll speeds examined.

Introduction

The horizontal twin roll casting process combines casting and hot ·lling into a single process which produces aluminum alloy strip directly ·om molten metal. As shown in Figure 1, molten metal is delivered between ·o water-cooled rolls using a set of ceramic casting tips, and begins to ·eeze upon contact with the rolls. Hot rolling begins once the strip has ·mpletely solidified. Heat is extracted from the strip over the arc of ·ntact extending from the end of the caster tip to the centerline of the ·lls.

The primary advantages of the roll casting process are high cooling ·tes and the ability to bypass conventional ingot hot rolling processes. A ·jor disadvantage is that productivity falls well below the theoretical ·tes dictated by the heat transfer limits for the process. The principal ·urces of these productivity limitations are roll-sheet adhesion (sticking) ·d the development of casting defects at higher casting speeds.

The key to understanding and curing the problems in roll casting lies · the ability to determine the thermal and mechanical conditions that exist ·thin the strip and at the roll-strip interface in the roll gap region. his paper discusses a simple thermomechanical model for the roll casting ·ocess which can be used to predict the temperatures and stresses that ·ist within the roll gap.

GA 16024.1

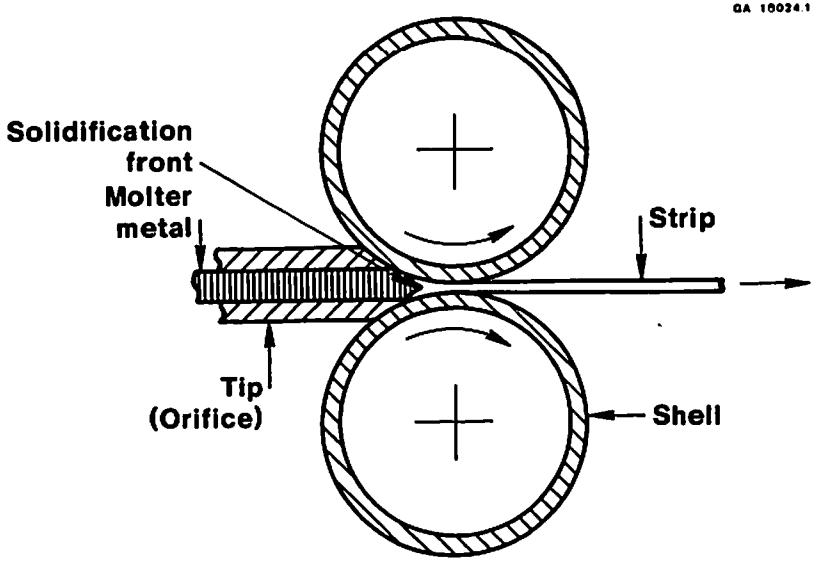

Roll Casting Schematic
Figure 1

The Model

The roll casting model consists of two separate, but fully coupled segments: a solidification segment and a hot rolling segment. Macromechanical variables, such as roll separating force, roll torque, and strip exit speed, can be predicted from the model given a knowledge of the roll shell temperature, interfacial heat transfer coefficient, coefficient of friction at the roll-strip interface, and the appropriate physical, thermophysical, and thermomechanical properties of the alloy being roll cast. These macromechanical variables provide the means for testing the validity of the model since they are easily measured.

When agreement between the predicted macromechanical values and experimental values is obtained, the model can be employed to extract information about the stresses and temperatures that exist within the roll gap.

Modeling Assumptions

A number of assumptions have been made in both the solidification and hot rolling models in order to provide a simplified model of the roll casting process. The solidification solution is independent of the rolling solution, except when the deformed roll radius in the hot rolling solution is excessive. In this case, the solidification solution is recalculated. The thermal solution employed is two-dimensional and edge effects are neglected. Heat generation due to plastic deformation and interface friction is neglected in the solidification solution.

The solidification solution includes alloy solidification but neglects convection in the liquid and within the mushy zone. Density is assumed to be independent of both phase and temperature in the continuity equation. Other properties, such as specific heat and thermal conductivity, differ for each phase but are independent of temperature.

Once solidification through the thickness of the roll gap is completed, the hot rolling model is activated. The thermal and mechanical solutions in the hot rolling model assume temperature independent material properties, with the exception of flow stress. The flow stress is assumed to be dependent on the average through-thickness temperature of the strip and the through-thickness strain rate. Work due to plastic deformation is assumed to be converted into heat.

The mechanical solution in the rolling portion of the process is based on the slab method of analysis. The pertinent assumptions here are:

* homogeneous through-thickness deformation
* plane strain
* circular arc of contact during roll deformation
* negligible inertial effects

Hence, the problem has been reduced to a two-dimensional thermal solution coupled with a quasi-static one-dimensional mechanical solution.

Solution Procedure

The details of the model have been presented in reference 1 for a pure substance. A brief summary of the solution procedure is given below. For the case of alloy solidification, a complete explanation of the model is presented.

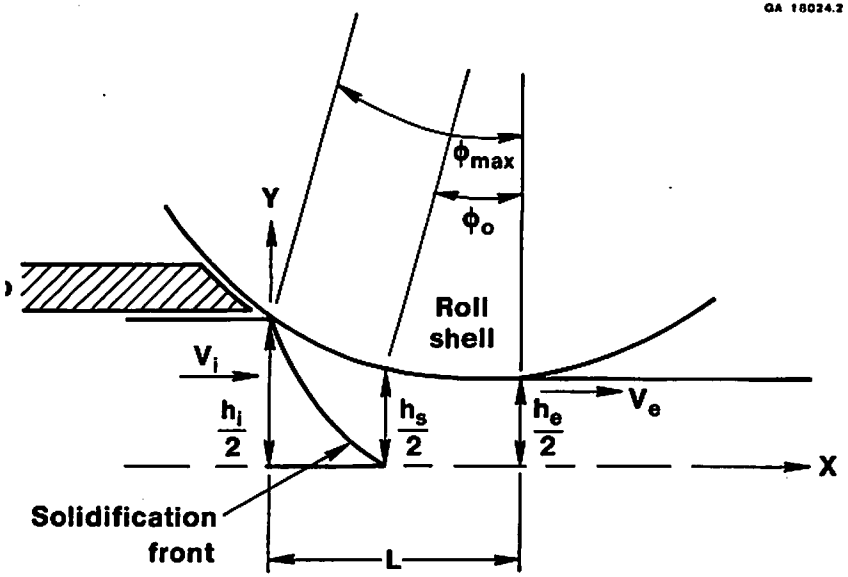

Eulerian Frame of Reference for Steady State Problem
Figure 2

Solidification Model

The governing energy equation is:

$$\rho c \frac{DT}{Dt} = \nabla\cdot(K\nabla T) + Q_{gen} \tag{1}$$

Considering the steady-state formulation in an Eulerian reference frame (see Figure 2), assuming that reduction in the gap remains small and keeping only the most important terms in each direction leaves:

$$\rho c V_x \frac{\partial T}{\partial X} = K \frac{\partial^2 T}{\partial y^2} \tag{2}$$

The corresponding continuity equation is:

$$V_x h = \text{constant} \tag{3}$$

where the velocity and height are sole functions of x.

The thermal boundary condition at the roll-strip interface is presented as a convective process, and is of the form:

$$-K \left.\frac{\partial T}{\partial y}\right|_{y=r} = h_c(T_r - T_R) \tag{4}$$

where h_c is a specified heat transfer coefficient, the subscript r refers to the strip surface, and R refers to the roll surface. The boundary condition at x=0 (at the nozzle inlet) normally fixes the inlet temperature at a specified value. However, a temperature distribution can also be specified at the inlet.

In the pure substance model described previously, the latent heat is released at a single temperature. The governing equation at the solidification front is:

$$Q_F \rho V \frac{dy}{dx} = K_s \frac{\partial T_s}{\partial y} - K_L \frac{\partial T_L}{\partial y} \tag{5}$$

where Q_F is the latent heat of fusion and the subscripts s and L refer to the solid and liquid sides of the interface, respectively.

For the alloy solidification model, the latent heat is released in segments within the freezing range at a finite number of specified temperatures. Between any two specified temperatures in the freezing range, the material properties are kept constant. The material properties in each mushy zone are averaged from the solid and liquid properties, using the fraction of the total latent heat release to define the fraction of solid and liquid within each zone. The equation used for alloy solidification is identical to equation 5, except that the subscripts s and L are replaced by i and i-1 to specify adjacent mushy zones and Q_F is replaced by Q_{Fi} to represent the fraction of the total latent heat released in the ith mushy zone.

The solution to the equations is found numerically using a finite difference marching procedure. By knowing the temperature at any x location, the temperatures at $x + \Delta x$ are found by using a central difference expression at x to determine $\partial^2 T/\partial y^2$ (equation 2). This determines $\partial T/\partial x$, and allows the temperatures at $x + \Delta x$ to be found by explicit integration.

Because of the solution procedure, it is necessary to estimate the thermal solution each time the solution front enters a regime with different material properties (a new mushy zone). This problem arises because the temperature derivatives are not continuous across the lines where fractions of the latent heat are released. For a small "seed" region in the newest mushy zone, the temperature and freeze-front locations are represented by:

$$T_{(x,y)} = a_o + a_1 y + a_2(y^2 + 2\alpha x) + \ldots + a_7(y^7 + 42\alpha y^5 + 420\alpha^2 y^3 x^2 + 840\alpha^3 y x^3 \tag{6a}$$

$$y_1(x) = b_1 x + b_2 x^2 + b_3 x^3 \tag{6b}$$

where x is the distance from the newest mushy zone, x_i, y is the distance from the roll surface, α is the thermal diffusivity of the zone ($\alpha = k/\rho c$), and the a's and b's are constants. The constants are evaluated by equating like powers of x in equations 4 and 5, and 6 at a predefined mushy zone temperature, $T(x,y_1)$. As a first approximation, the temperature gradient in equation 5 at mushy zone (i-1) is set equal to a constant, c_o, where:

$$c_o = \left.\frac{\partial T_{i-1}}{\partial y}\right|_{y=0,\ x=x_i}$$

This seed solution is used until the temperature prediction, T_i, ates from the predefined mushy zone temperature, $T(x,y_i)$ by a specified int; then the finite difference procedure is employed. In subsequent :ations for the mushy zone seed calculation, temperatures in the (i-1)th : are used to calculate a quadratic expression in x for

$$\left.\frac{\partial T_{i-1}}{\partial y}\right|_{y=y_i}$$

ch is then used in equation 5.

Results produced by the previously described solution technique have n compared to results from a commercial finite element code, ABAQUS,[2] for pecial class of problems. ABAQUS can be used to analyze a -dimensional transient conduction problem with constant coefficients. By ving the roll casting problem with a large roll radius and small uction, equation 2 becomes equivalent to the ABAQUS problem, since v_x is irly constant and x/v_x is equivalent to time.

Figures 3 and 4 demonstrate the rate of convergence of the two :hniques as a function of the number of mushy zones employed in the model. ;ure 3 compares the strip surface temperature predictions of the two :hniques at complete solidification for three different cases (the)script M refers to the model, A refers to ABAQUS). Case 1 uses a 100°F le mushy zone and a uniform release of latent heat over the temperature ıge. Case 2 is identical to case 1, except that the width of the mushy ıe has been doubled. Case 3 uses a 100°F wide mushy zone, but releases e latent heat as a quadratic function of temperature in the mushy zone. ses 1 and 2 converge to the ABAQUS result, while case 3 appears to nverge to a slightly lower temperature. Figure 4 compares the predicted eeze-front locations for the same three cases. The convergence results e the same, except that convergence occurs more quickly.

Hot Rolling Model

The hot rolling model is identical to the one described in reference 1. consists of a fully coupled thermomechanical solution.[3] The governing ergy equation is identical to the one used in the solidification model, uation 2, with the exception that a heat generation term is included:

$$\rho c V_x \frac{\partial T}{\partial x} = K \frac{\partial^2 T}{\partial y^2} + Q_{gen} \qquad (7)$$

Heat generation comes from two mechanical sources: plastic deformation f the metal and friction at the interface between the roll and the)rkpiece.

The mechanical equilibrium equation is derived by the slab method. his method and the contributions made by a number of authors are summarized y Alexander.[4] Under plane strain conditions, the governing equation ecomes:

$$\frac{ds}{d\phi} = sg(\phi) + f(\phi) \qquad (8)$$

here s is the normal roll pressure, ϕ measures the distance into the roll ite (ϕ = sin [(L-x)/R]), and f and g are functions which depend on the flow

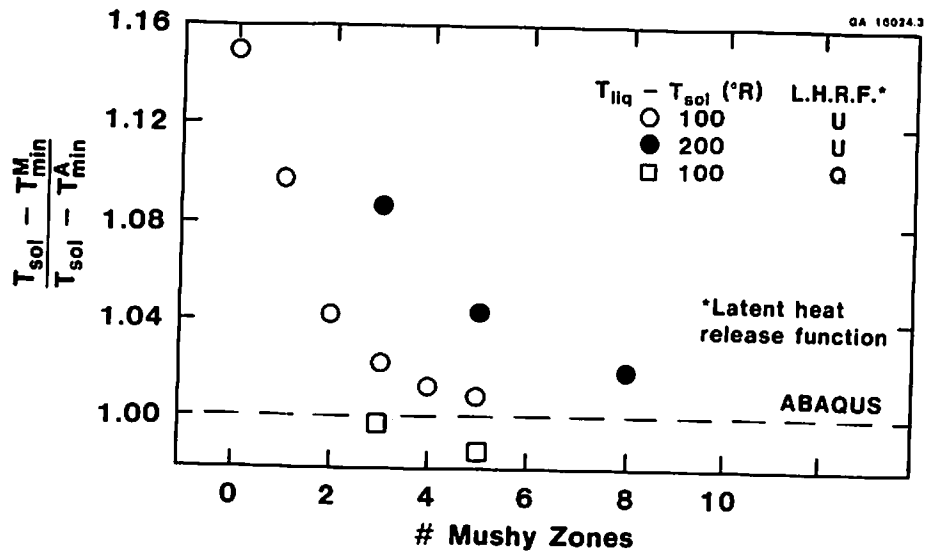

Interface Temperature at Complete Solidification
Figure 3

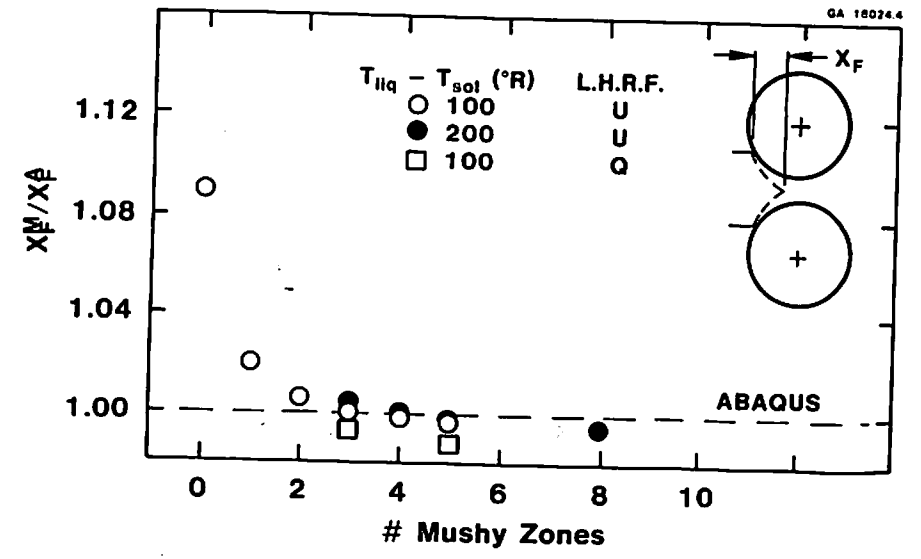

Freeze Front Location
Figure 4

ress and the interfacial shear stress. The uniaxial flow stress, σ, is pressed as a function of temperature and strain rate, in the form veloped in reference 5:

$$\sigma = \left(\frac{1}{\lambda}\right) \ln \left[(D/A)^{1/n} + \left([D/A]^{2/n} + 1\right)^{1/2}\right] \qquad (9a)$$

ere,

$$D = \dot{\epsilon} \exp \left[\Delta H/(\bar{R}T)\right] \qquad (9b)$$

is the universal gas constant, and λ, ΔH, A, and n are material operties.

Experimental Procedure

A pilot scale horizontal roll caster with 14 inch diameter water-cooled eel shells was used to test the model. The caster was equipped with a mputerized data logging system to monitor a number of parameters, cluding caster torque, roll speed, strip exit speed, molten metal mperature at the inlet basin, metal level at the inlet basin, and strip it temperature.

Experimental data was collected by the following procedure: First, the ll speed was adjusted to the desired value. The speed was held until all nitored parameters stabilized, and then data was recorded at intervals of second over a 5 minute period. At the end of the data collection cycle, e roll speed was increased by approximately 2 inches/minute and the ocess was repeated.

The total caster torque was determined from voltage, current, and roll eed data that was recorded at each interval. The net torque was termined by subtracting the torque obtained by the same technique under -load conditions (no metal in the roll bite) from a separate test.

The molten metal supply was sufficient to allow several hours of peration. This ensured that sufficient casting time was available to hieve steady-state operating conditions after each incremental speed hange.

Experimental Results

Experiments on the roll caster were performed with a 3000 series alloy or roll surface speeds ranging from 30 to 53 inches/minute. The alloy was oll cast to produce a strip approximately 6 inches wide and 0.160 inches hick. The actual width and thickness of the strip was determined from mples taken at each casting speed. Strip width increased slightly with ncreasing roll speed, while the strip thickness decreased.

The effects of roll speed on the exit temperature of the strip, the net aster torque, and the strip exit speed were also determined. As the roll peed is increased, the solid-liquid interface is shifted closer to the enterline of the rolls, resulting in an increase in strip exit temperature nd a drop in net caster torque, as shown in Figures 5 and 6, respectively. he difference between the strip exit speed and the roll surface speed also ncreases with roll speed, as shown in Figure 7.

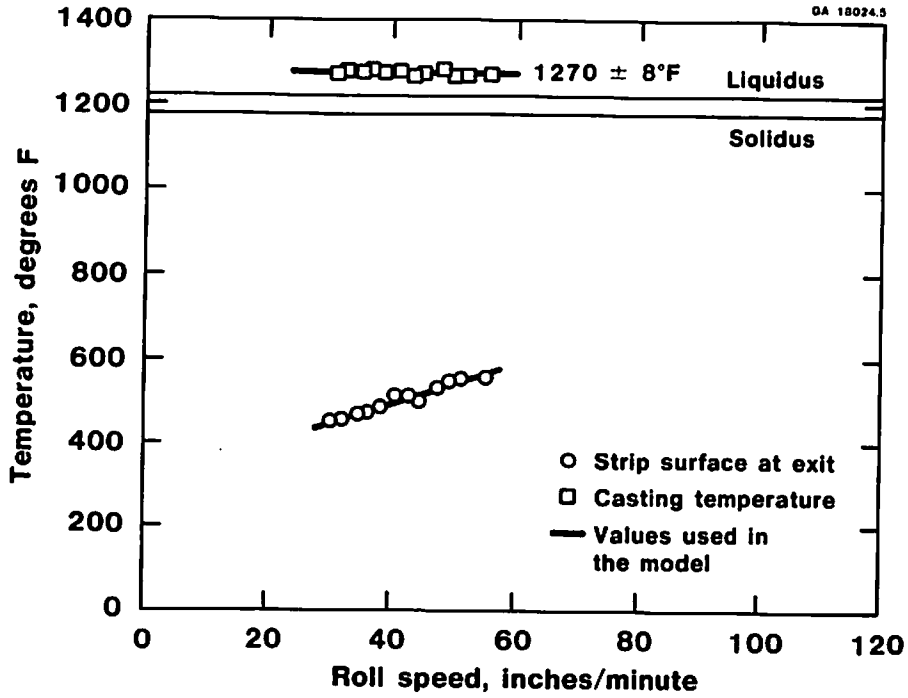

Strip Exit Temperatures vs. Roll Speed
Figure 5

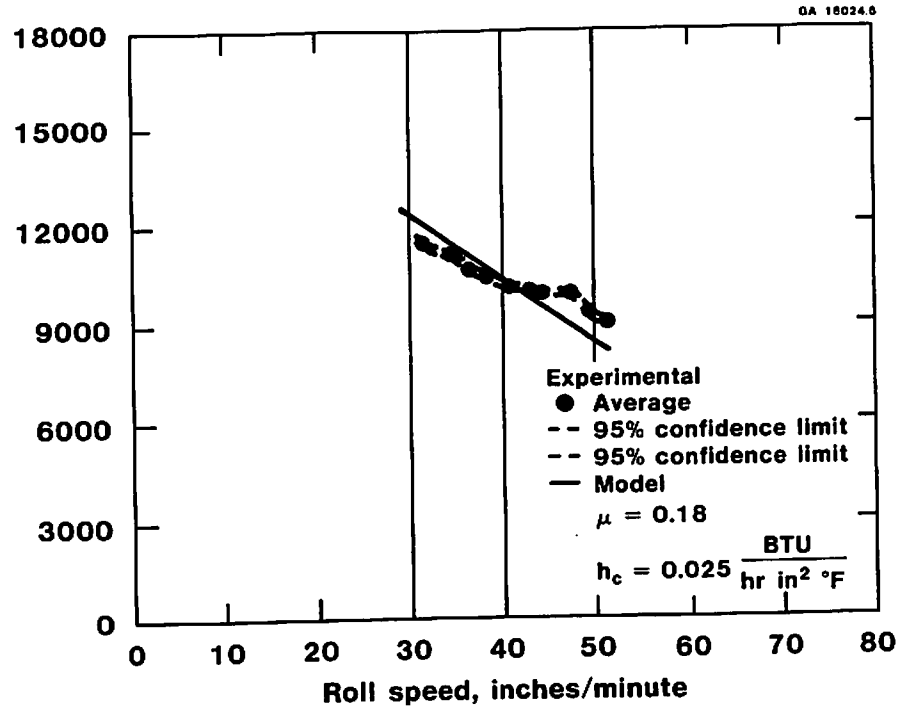

Net Caster Torque vs. Roll Speed
Figure 6

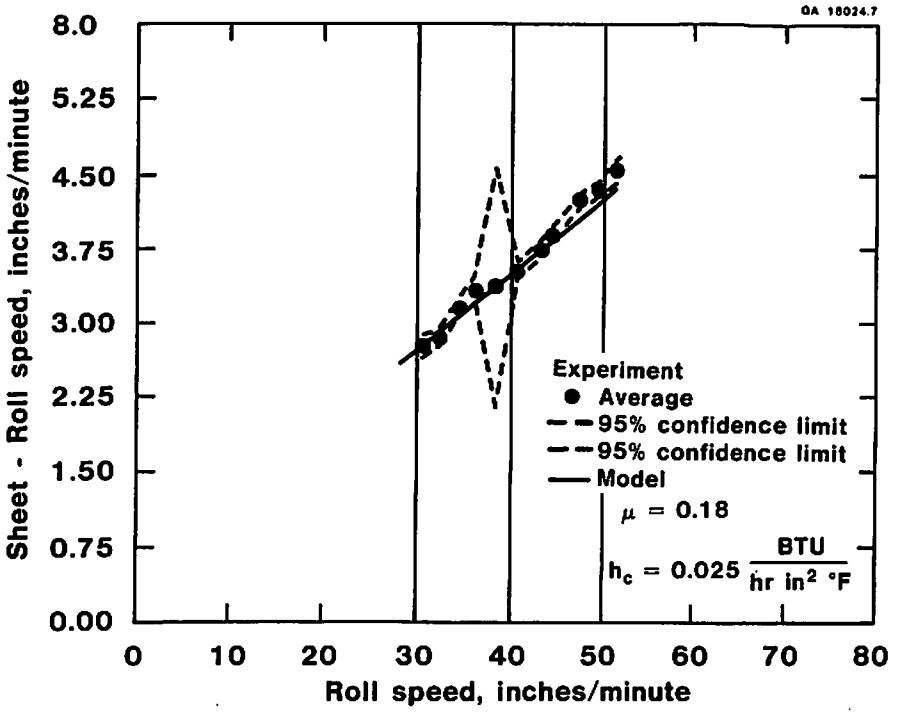

Strip-Roll Slip Velocity at Exit vs. Roll Speed
Figure 7

Comparison

In order to compare model predictions with the experimental results from the tests with the 3000 series alloy, the observed dependence of strip width and thickness on roll speed were utilized as inputs to the model. After supplying the appropriate physical, thermophysical, and thermomechanical inputs to the model, three inputs that are not readily specified remain: the roll temperature, the interfacial heat transfer coefficient, and the coefficient of friction at the roll-strip interface.

To test the ability of the model to predict experimental observations for various combinations of the three unspecified inputs, roll temperatures were chosen to force agreement between predicted and experimental strip exit temperatures over the entire range of roll speeds. Then the heat transfer coefficient and the coefficient of friction were chosen to force agreement with the experimental net caster torque at a single reference roll speed (40 inches/minute). Since various unique combinations of heat transfer coefficient and coefficient of friction could reproduce the experimental torque at the reference speed, the single combination that also reproduced the experimental strip exit speed at the reference roll speed was chosen as the best estimate for the interfacial heat transfer coefficient and the coefficient of friction.

The best overall agreement between experimental and predicted torque l strip exit speed at the reference roll speed occurred when $\mu = 0.18$ and $= 0.025$ BTU/hr-in^2-R (73.6 kJ/m^2-s-K). A comparison of the predicted and perimental torques and sheet speeds for the entire range of roll speeds is own in Figures 6 and 7, respectively. As seen in these figures, the model edicts a slightly greater drop in net torque with roll speed than is served experimentally. The maximum difference between experimental and edicted torques is about 8 percent. The predicted and experimental exit ip velocities agree to within 3 percent.

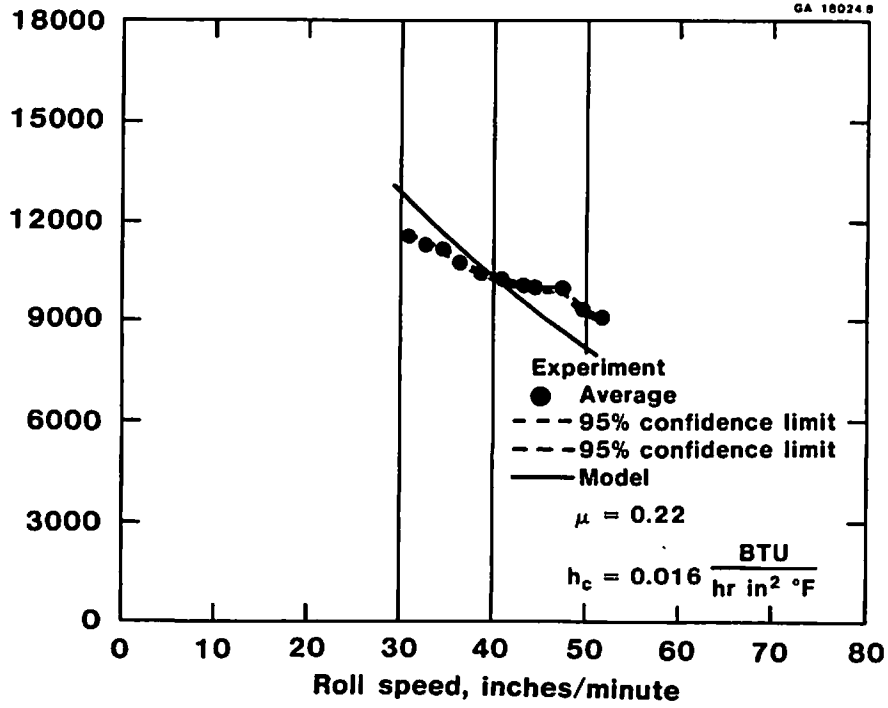

Net Torque Predictions Using Higher μ Value
Figure 8

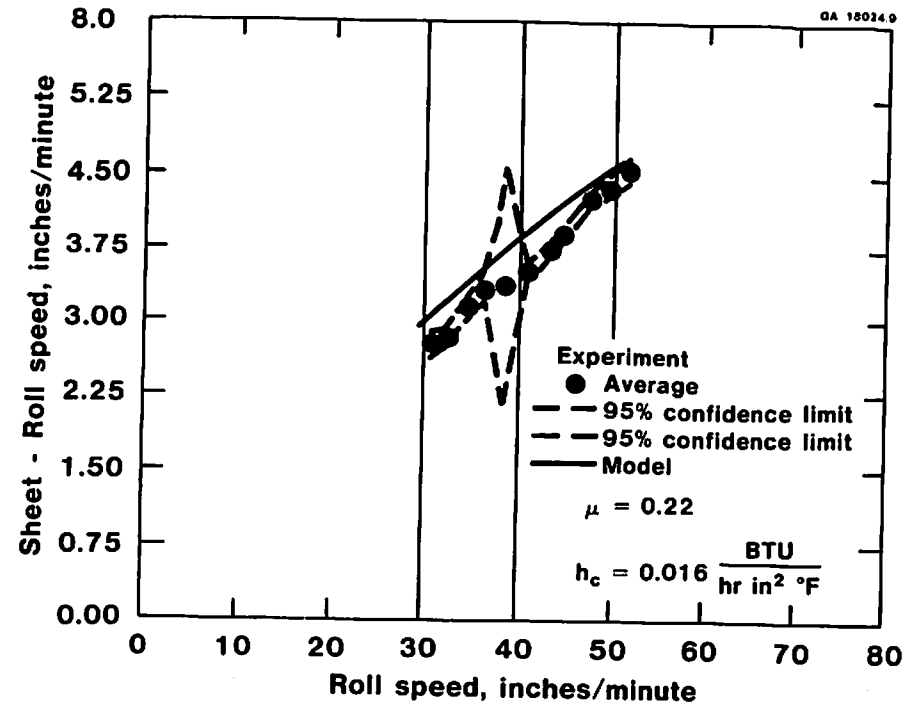

Sheet-Roll Slip Predictions Using Higher μ Value
Figure 9

The sensitivity of the model to choices of μ and h_c is demonstrated in Figures 8 to 11. These figures show other combinations of μ and h_c that force agreement with net caster torque at the reference speed. For higher values of μ and lower values of h_c (Figures 8 and 9), the predicted exit slip velocity is high and the agreement between the predicted and observed roll speed dependence of the torque is worsened. For lower values of μ and higher values of h_c (Figures 10 and 11), predicted exit slip velocities are low, but the predicted speed dependence of the torque improves. However, the value for h_c is unreasonably large in this case.

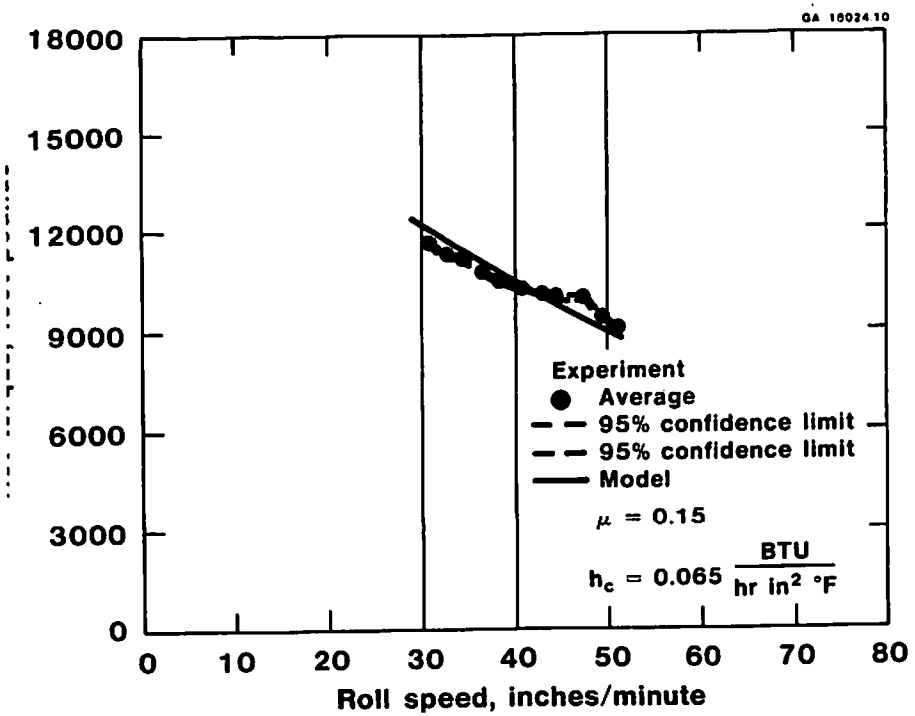

Net Torque Prediction Using Lower μ Value
Figure 10

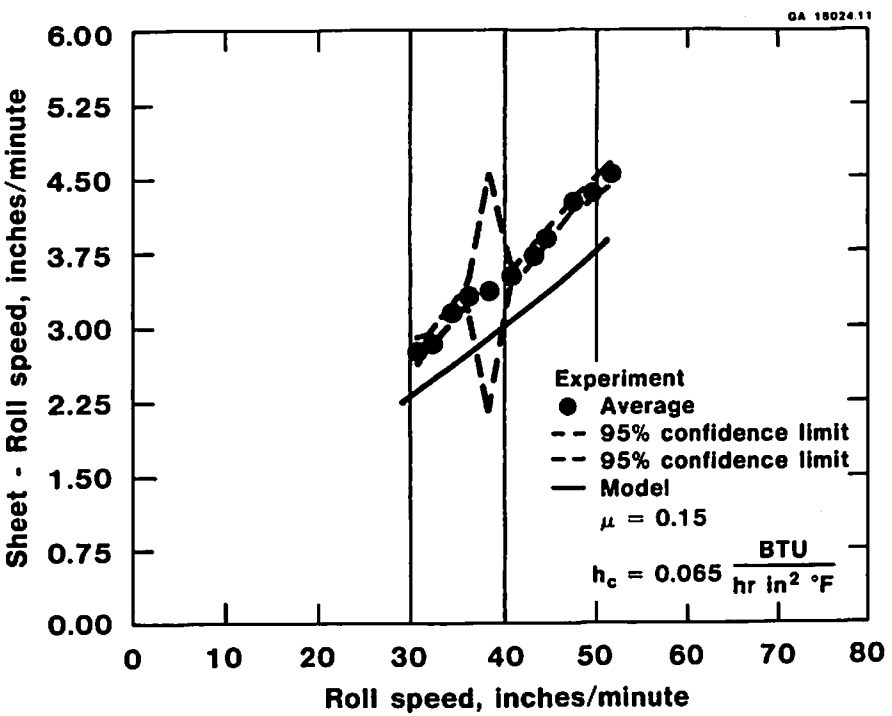

Sheet-Roll Slip Predictions Using Lower μ Value
Figure 11

While the values of μ and h_c used to generate Figures 6 and 7 are elieved to best represent the range of observed experimental values, iditional experimental information will be required to confirm the choice f h_c and μ. Measurements of separating force and freeze-front position are lanned in the future to provide additional means of testing the validity of ie model and the validity of the choices of μ and h_c.

Model Predictions

Using the "best fit" values of μ and h_c, the model has been employed to redict stress, temperature, and freeze-front location within the roll bite. ie predicted shear stress distribution along the interface between the roll id the solidified strip is shown in Figure 12 for roll speeds of 30, 40, id 50 inches/minute. For the casting conditions employed in the present xperiments, the model predicts that the interfacial shear stress remains elow the plane strain yield stress of the alloy along the entire roll-strip nterface ("sticking friction" conditions are not encountered). The maximum tress, which marks the neutral point in the roll bite (the point where the trip and roll speeds are equal), decreases with increasing roll speed and s shifted slightly toward the exit of the roll bite as roll speed is ncreased.

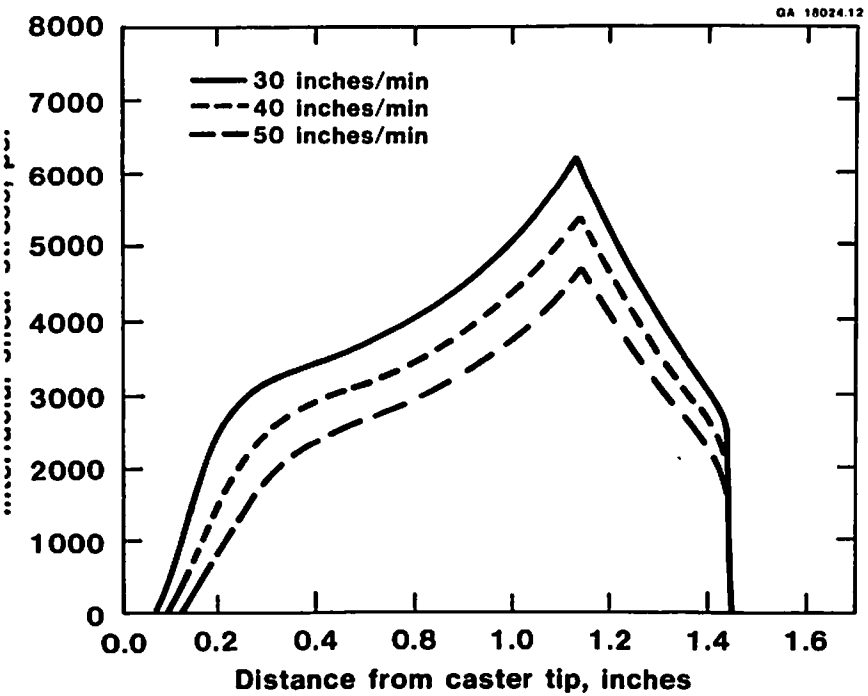

Predicted Interfacial Shear Stress Distributions for Three Roll Speeds

Figure 12

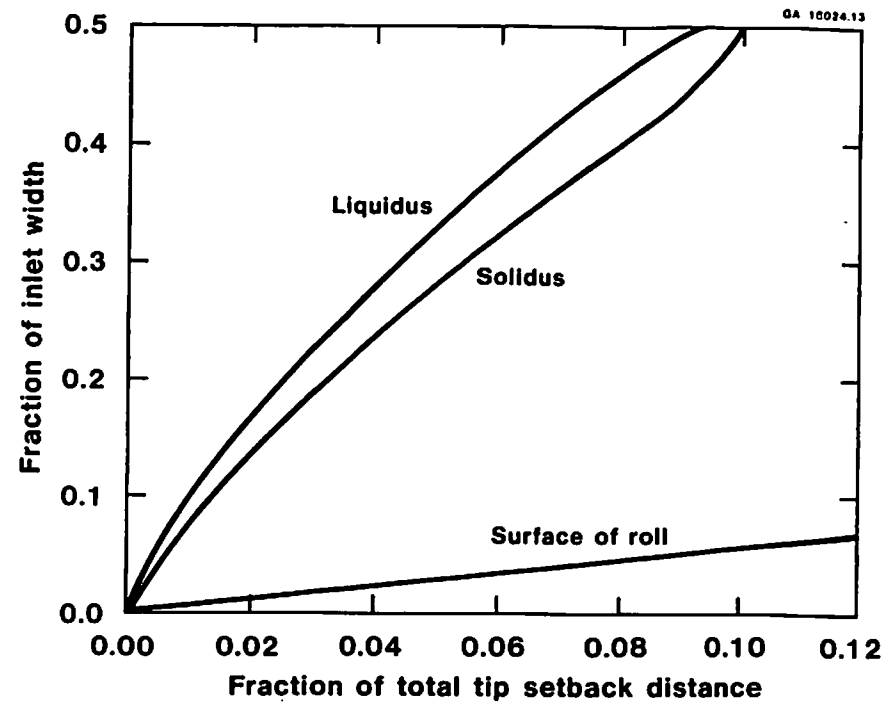

Predicted Shape of the Freeze Front at a 40 Inch/Minute Roll Speed

Figure 13

The point at which the interfacial shear stress for each roll speed first rises above zero in Figure 12 marks the point of complete through-thickness solidification for that roll speed. For the conditions reported here, this sump depth is only a small part of the total length of roll-strip contact. Short sump depths have also been observed by other investigators.[6,7] Also, predicted change in freeze-front location with roll speed is small; on the order of 0.03 inches/inch/minute change in roll speed. A more detailed prediction of the shape of the freeze-front is shown in Figure 13 for a roll speed of 40 inches/minute.

Predictions of the temperatures at the surface and center of the solidified strip within the roll bite are shown in Figure 14 for a roll speed of 40 inches/minute. At the point of complete through-thickness solidification, the temperature difference from surface to center is predicted to exceed 200°F. However, the surface and center temperatures of the strip converge rapidly and reach a constant temperature at about one third of the way through the roll bite. At the exit to the roll bite, the strip temperature has dropped to within 1°F of the imposed roll shell temperature for the range of experimental conditions described above.

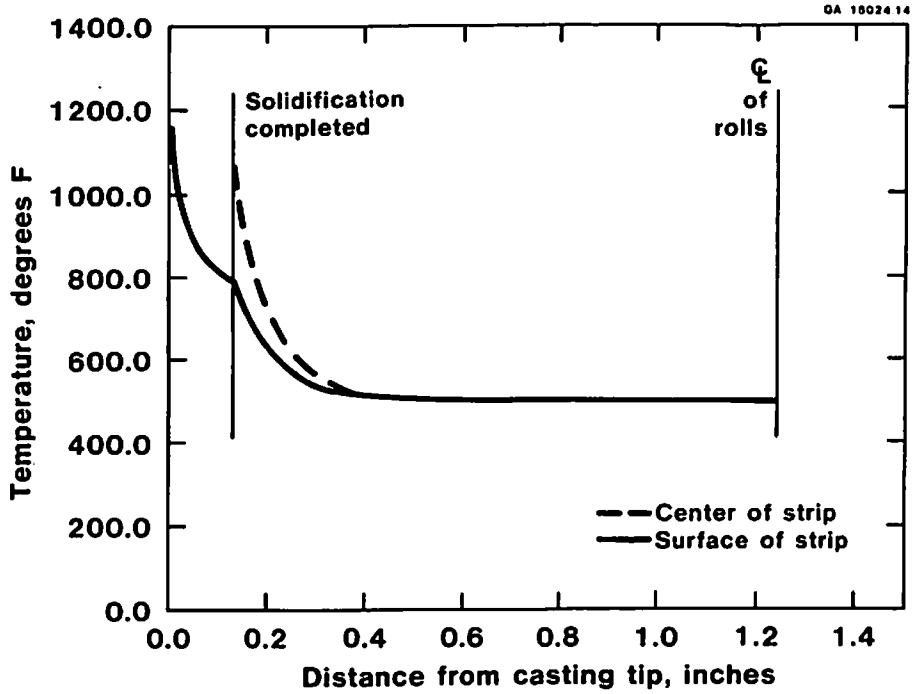

Predicted Temperature of the Solid Strip at a 40 Inch/Minute Roll Speed

Figure 14

Summary

A simulation of the roll casting process has been developed which combines a casting model and a hot rolling model to predict measurable process responses such as net caster torque and strip exit speed, and internal information such as interfacial shear stress distribution, temperature distribution, and freeze-front location within the roll gap.

Using experimentally determined strip exit temperatures as input to the model, and forcing agreement between experimental and predicted caster torque and strip exit speed at a single reference speed, values for the coefficient of friction ($\mu = 0.18$) and the interfacial heat transfer coefficient ($h_c = 0.025$ BTU/hr-in^2-°F) were obtained. Results from the model were shown to be in good agreement with experimental torque and strip exit speeds for the entire range of roll speeds examined. The model was then employed to predict interfacial shear stress, temperature distribution, and freeze-front location for the reported experimental conditions.

Nomenclature

A	material constant (1/s)
a, a_0, a_1 . . .	constants used in temperature approximation
b_1, b_2, b_3	constants used in solidification front expression
c	specific heat (J/Kg/°C)
c_θ	temperature gradient (°C/m)
ΔH	material constant (J/mol)
h_c	heat transfer coefficient (J/m^2/s/°C)
h	strip height in roll bite (m)
h_i, h_s, h_e	strip heights at entrance, complete solidification, and exit (m)
K	thermal conductivity (J/m/s/°C)
L	strip-roll contact length (m)
n	material constant
Q_F	heat of fusion (J/kg)
Q_{Fi}	fraction of heat of fusion released at temperature T_i
Q^{gen}	heat generation terms
R, $\bar{R}$	undeformed and deformed roll radii (m)
R	universal gas constant (J/mol/°K)
s	normal stress between strip and roll (Pa)
T	temperature (°C or °K)
T_i	specified temperature times within freezing zone
V_i, V_e	entrance and exit strip velocities (m/s)
V_r	surface velocity of roll (m/s)
V_x, V_y	x, y velocity components of strip (m/s)
Y_i	front position of temperature time T_i (m)
α	$K/(\rho c V_x)$ (m)
$\dot{\epsilon}$	strain rate average through-thickness (1/s)
λ	material constant (1/Pa)
μ	Coulomb friction factor
ρ	density (kg/m^3)
σ	flow stress (Pa)
ϕ	angular position on roll as measured from exit plane
ϕ_{max}	total contact arc
ϕ_o	total contact arc of complete solidification
ψ	velocity difference between roll surface and strip (m/s)
Ψ	normalized ψ (%)
ω	angular velocity of roll (rad/s)
P_e	Peclet number

References

- M. E. Karabin and R. E. Smelser, "A Simplified Thermomechanical Model of Roll Casting," (Paper 85-WA/HT-34 presented at ASME 1985 Winter Annual Meeting).
- D. Hibbitt, B. Karlsson, and E. P. Sorensen, ABAQUS User's Manual, Providence, Rhode Island (1984).
- M. R. Tharrett, "A Coupled Thermal-Mechanical Model and Experimentation of Hot Rolling" (Master's thesis, University of Pittsburgh, 1983).
- J. M. Alexander, "On the Theory of Rolling," Proc. R. Soc. Lond. A.326, 535-563 (1972).
- T. Sheppard and D. S. Wright, "Determination of Flow Stress: Part I - Constitutive Equation for Aluminum Alloys at Elevated Temperatures," Metal Technology, 215, 1979.
- R. Iricibar and I. Jin, "Rolling Aspects of Twin Roll Casting," pp. 1129-1144, Light Metals 1984, J. J. Miller, ed.; AIME, New York, N.Y., 1984.
- S. J. Bercovici, "Optimization of 3C Roll Caster by Automatic Control," pp. 1285-1299, Light Metals 1985, H. O. Bohner, ed.; AIME, New York, N.Y., 1985.

MODELING OF A TWIN-BELT STRIP CASTING PROCESS*

Y.G. Kim, B. Farouk and D. Apelian

Drexel University
College of Engineering
Philadelphia, Pennsylvania 19104

Abstract

Continuous strip casting has received considerable attention in recent years due to its economic advantages with increased energy savings and the elimination of intermediate processing steps. A promising concept in strip casting is the twin-belt (Hazelett) process which incorporates two cooled continuously moving thin metal belts wrapped around pulleys which tension and drive the belts at a predetermined speed. Molten metal is introduced at the entry end of the caster through a tundish and feeding nozzle into the mold. The twin-belt process has been successfully used with non-ferrous metals such as aluminum, copper and brass, and is a prime candidate for strip casting of ferrous materials. A numerical model has been developed which predicts the interface locations, the temperature fields in the solid and liquid regions of the cast and the velocity fields of the liquid metal at the entrance region of the twin-belt caster. The process variables considered are the velocity and cooling conditions of the belt and the nozzle shape. A body fitted coordinate system is used to track the front locations and to solve the Navier-Stokes equations in the liquid region. Results obtained can help design efficient casters for thin strip steel castings. The development of the numerical model is presented, and sample results are discussed.

* Paper submitted for presentation at Third International Modeling of Casting and Welding Processes, Santa Barbara, California, January 13-17, 1986.

Modeling and Control of CASTING AND WELDING PROCESSES

Proceedings of the Third Conference on Modeling of Casting and Welding Processes sponsored by the Engineering Foundation. It was held on January 12-17, 1986 in Santa Barbara, California.

Edited by

Sindo Kou
University of Wisconsin-Madison
Madison, Wisconsin

Robert Mehrabian
University of California
Santa Barbara, California